



NATIONAAL INSTITUUT VOOR KERNFYSICA EN HOGE-ENERGIEFYSICA

NIKHEF/AmPS/89/03



**NIKHEF-K CONTRIBUTIONS TO
THE 1989 PARTICLE ACCELERATOR CONFERENCE
CHICAGO, MARCH 20-23, 1989**

The Amsterdam Pulse Stretcher Project

G.Luijckx, J.H.M.Bijleveld, H.Boer Rookhuizen,
P.J.T.Bruinsma, A.P.Kaan, F.B.Kroes, L.N.Kuijjer, R.Maas,
J.G.Noozen, J.C.Post, J.B.Spelt, C.de Vries

Optics of the Amsterdam Pulse Stretcher

R.Maas, Y.Y.Wu

**Modification of MEA modulator-klystron units enabling
short pulse injection into a pulse-stretcher ring**

F.B.Kroes, E.Heine

Performance and Modification of the MEA R.F. Drive System

F.B.Kroes, T.G.B.W.Sluyk, B.Hautenik

**An Energy Spectrum Compressor System for
the Amsterdam Pulse Stretcher**

J.G.Noozen, R.Maas

NIKHEF - K - Amps -- 89 - 03 .

**NIKHEF-K CONTRIBUTIONS TO
THE 1989 PARTICLE ACCELERATOR CONFERENCE
CHICAGO, MARCH 20-23, 1989**

The Amsterdam Pulse Stretcher Project

G.Luijckx, J.H.M.Bijleveld, H.Boer Rookhuizen,
P.J.T.Bruinsea, A.P.Kaan, F.B.Kroes, L.H.Kuijjer, R.Maas,
J.G.Noozen, J.C.Post, J.B.Spelt, C.de Vries

Optics of the Amsterdam Pulse Stretcher

R.Maas, Y.Y.Mu

**Modification of MEA modulator-klystron units enabling
short pulse injection into a pulse-stretcher ring**

F.B.Kroes, E.Heine

Performance and Modification of the MEA R.F. Drive System

F.B.Kroes, T.G.B.W.Sluyk, B.Hautenik

**An Energy Spectrum Compressor System for
the Amsterdam Pulse Stretcher**

J.G.Noozen, R.Maas

THE AMSTERDAM PULSE STRETCHER PROJECT (AmPS).

G. Luijckx, J.H.M. Bijleveld, H. Boer Rookhuizen,
P.J.T. Bruinsma, A.P. Kaan, F.B. Kroes, L.H. Kuijter,
R. Maas, J.G. Noomen, J.C. Post, J.B. Spelt, C. de Vries

NIKHEF-K
P.O.Box 4395, 1009 AJ Amsterdam, The Netherlands

SUMMARY

To obtain electron beams with a high duty factor a stretcher and storage ring will be added to the existing Medium Energy Accelerator (MEA) facility. The ring will operate at energies between 250 and 900 MeV and with circulating currents up to 200 mA. The storage mode will be used for internal target physics.

INTRODUCTION

The present 500 MeV, 1% duty factor electron linac facility MEA [1] has been in continuous operation since 1980. MEA is primarily used for electron scattering experiments of the (e,e'p) type. Coincidence measurements are an essential part of these experiments. The real/random ratio of coincidences is proportional to the duty factor (d.f.). To enhance the efficiency of the experiments a proposal was submitted in 1984 to increase the d.f. to > 90 % by adding a pulse stretcher to the facility [2]. End of 1987 this proposal has been approved by the funding agencies. Meanwhile it was decided to use the ring in a storage mode as well to allow experiments with internal targets (IT). To achieve an acceptable luminosity currents up to 200 mA will have to be stored. In addition to these requirements the maximum energy has been increased as well. To reduce the costs of the project the circumference of the ring was reduced from the original 280 m to 212 m. In order to maintain an acceptable extracted current on target the maximum peak current of the linac had to be increased to 80 mA assuming a 3 turn injection. A comparison of the present and future modes is made in Table 1.

BASIC RING DESIGN

LAYOUT: Fig.1 shows the layout of the ring and the experimental areas. Existing vaults will accommodate 100 m of the ring. For the remaining 112 m a new tunnel will be built. Part of the tunnel will be combined with a new experimental hall for internal target physics.

Table 1. Comparison of main beam parameters on target, present mode and in stretcher & storage mode.

	Present	Stretcher	Storage
E min [MeV]	75	250	300
E max @ i= 80 mA [MeV]	550	700	900
E max @ i=0 [MeV]	580	910	910
Linac pulse [μsec]	40	2.1	2.1
Rep. rate [Hz]	300	400	-
Beam d.f. [%]	1.2	>90	100
Peak i MEA [mA]	10	80	10
Target <i> [μA]	>100	67	200000

LATTICE: the ring is designed with a four fold symmetric lattice [3]. Each curve is a double achromat and consists of 8 dipoles, 8 quadrupoles and 8 sextupoles. The curves are connected by dispersion free straight sections each with a length of 32 m. The internal target, the RF cavities (one for each mode) and the injection and extraction septa are all located in straight

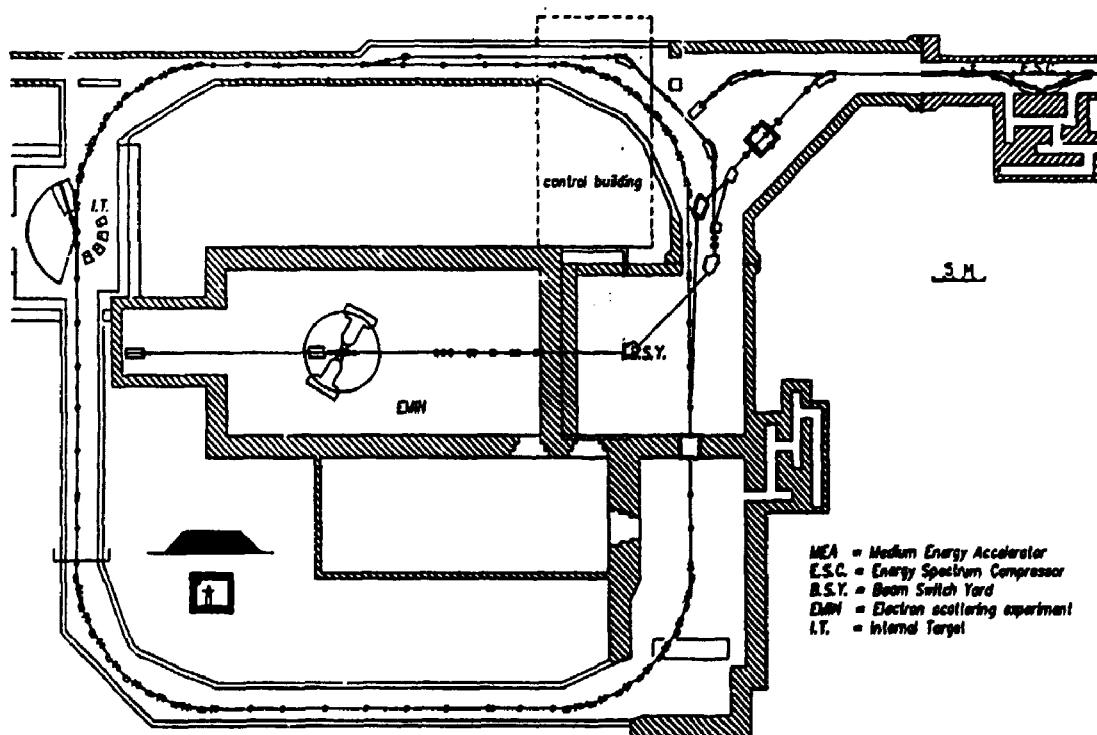


Fig.1 Layout of the ring; also shown are the end of the linac with the energy spectrum compressor (ESC), the beam switch yard (BSY), the electron scattering end station (EMIN) and the internal target hall (IT). The walls of the existing buildings are hatched.

sections (IT and RF at locations with small beta functions; injection and extraction at locations where the beta's are large). A list of machine parameters is presented in table 2.

Table 2. List of important machine parameters of AmPS.

Ring circumference	211.618	m	
Revolution frequency	1.417	MHz	
Beta function (maximum)	22.5	m	
Beta function (minimum)	2.0	m	
Dispersion function (maximum)	2.7	m	
Momentum compaction factor	0.027		
Tune in stretcher mode			
horizontal	7.637		
vertical	7.22		
Tune in storage mode			
horizontal	7.61		
vertical	7.15		
Chromaticity in stretcher mode			
horizontal	-15.0		
vertical	+0.2		
Chromaticity in storage mode			
horizontal	+0.2		
vertical	+0.2		
RF frequency (stretcher)	2.856	GHz	
harmonic number	2016		
Synchrotron radiation @ 9 GeV			
energy loss/turn	17.59	keV	
emitted power @ 0.2 A	3.52	kW	
critical energy	0.49	keV	
Damping times [msec], Touschek lifetimes [hr]			
Energy [MeV]	300	600	900
Damping time			
transversal	1944	243	72
longitudinal	977	122	36
Touschek lifetime	0.3	1.3	11.6
(100 % coupling, I=200 mA, RF=130 kV)			

INJECTION: 3 turn injection is foreseen; 2 fast electrostatic kickers deflect the closed orbit during injection. A d.c. injection septum will be used. In storage mode at energies > 700 MeV, because of beam loading (2.5 MeV/mA) in the linac, injection will require tens of pulses to achieve a circulating current of 200 mA. Third integer resonance extraction will be used [3].

STORAGE MODE: in this mode a thin dust or gas jet target will interact with the circulating beam. Target densities as high as $1 \text{ E } 17 \text{ atoms/cm}^2$ will be used. Lifetimes of the beam have been calculated taking into account the effects of Bremsstrahlung, single and multiple scattering and Møller scattering: for a hydrogen target the $1/e$ lifetime at 900 MeV & $1 \text{ E } 17 \text{ atoms/cm}^2$ is 30 sec, at 300 MeV & $1 \text{ E } 16 \text{ atoms/cm}^2$ it is 90 sec. [4]

To be sure that currents up to 200 mA can be stored the current thresholds for the single and coupled longitudinal bunch instability as well as the transversal instability are studied at present. First calculations show that stable operation should be possible with the chosen lattice. A separate RF cavity with a frequency < 500 MHz is planned for the storage mode.

RING HARDWARE

MAGNETS: all d.c. ring magnets are laminated both because of cost considerations and to improve their reproducibility. They can be split into 2 halves to ease the installation of the vacuum chambers. The coils of the ring dipoles are made of aluminium tape and they will be cooled indirectly. It is not yet sure of this type of coil can also be used for the quadrupoles and sextupoles. The dipoles and families of quadrupoles and sextupoles will be powered in series. Kickers and septa are still in an early design stage; special attention is given to an RF compatible design. Some specifications of magnets and septa are given in table 3.

Table 3. Specifications of ring magnets and septa. D : dipole, Qc : quadrupole curved section, Qs : quadrupole straight section, S : sextupole

Magnet type	D	Qc	Qs	S
Quantity	32	32	36	32
Field @ 1 GeV [T]	1	0.33	0.33	0.024
Gap/aperture [mm]	50	75	110	75
Homogeneity/ [0.1 %]	1.5	-	-	-
Harmonic content [%]	-	0.1	0.1	0.1
Length [mm]	647	212	297	212
Kickers:	electrostatic, length 1.6 m, 2 mrad deflect., flat pulse during 2.1 μ sec, fall time < 70 nsec, deflection voltage @ 1 GeV :+ & - 25 kV			
Septum :	injection: d.c., septum thickness 2 mm 20mrad deflection, field @ 1 GeV 0.167 T			
Septum :	extraction: electrostatic wire septum, wire thickness 0.1 mm, gap 20 mm, length 2 m, 5 mrad deflection, voltage @ 1 GeV 55 kV.			

VACUUM & MECHANICAL CONSTRUCTIONS: the required pressure is determined by the quantum lifetime in storage mode. Considering the decay of the beam intensity in the presence of an internal target (a few minutes) a quantum lifetime of one hour should be adequate. The vacuum system will be designed for a pressure (with beam) of $1 \text{ E } -6 \text{ Pa}$. The vacuum chambers and beam pipes will be made of stainless steel 316 LN. This choice has been made mainly because of the low manufacturing costs and the low initial pressure (especially when vacuum fired) when compared to aluminium [5]. The need for in situ bake out is still being investigated. Ion getter pumps will be used with a total capacity of 4000 liter/sec. All vacuum components will be designed with a smooth bore; RF shields will be fitted in bellows, pump outs, etc. Ring components, including magnets, will be pre-installed and pre-aligned on girders. Fig.2. shows a girder layout.

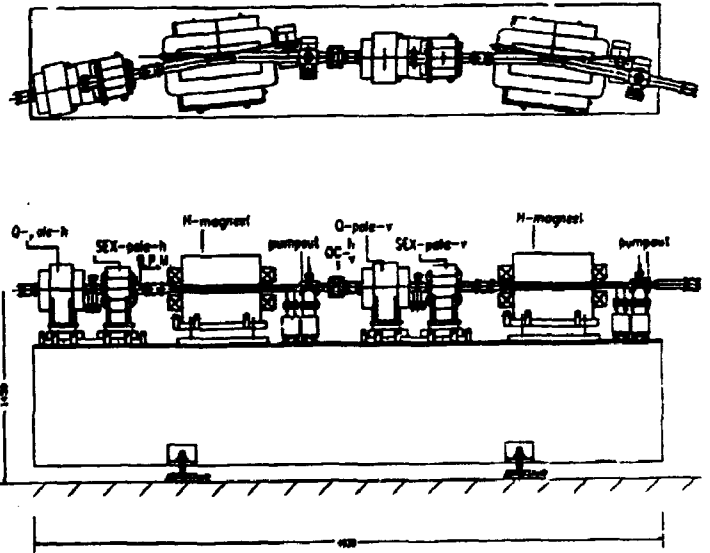


Fig.2. Part of curved section showing 2 dipoles, 2 quadrupoles and 2 sextupoles on the supporting girder

RF SYSTEM: in stretcher mode a cavity operating at the linac frequency of 2856 MHz will be used; this frequency was chosen to minimize the capture loss at injection. At 850 MeV the required RF voltage is 95 kV. Proper extraction control can be achieved by amplitude and phase modulation of the RF. A slow wave cavity structure enables this because of its broadband behaviour. Several CW klystrons are commercially available to power the cavity structure.

In storage mode a high overvoltage is required to insure a reasonable quantum lifetime; since for a given bucket size the RF power scales roughly to the harmonic number, it pays to lower the frequency. Until now operation at 476 MHz with a standing wave cavity is assumed. At 900 MeV an RF voltage of 110 kV will then be required.

DIAGNOSTICS: an overview of planned monitors is given in table 4.

Table 4. Listing of ring monitors and their resolution.

Parameter	qty	type	resolution
position	32	stripline	0.1 mm @ $I > 1$ mA
	8	synchr.radiation	1 mm
	8	screen	1 mm
profile		flying wire	<0.1 mm
current	1	d.c.transformer	0.1 mA; 10 kHz
	1	stripline	0.1 mA; 0.1 GHz
dE/E	2	synchr.radiation	0.03%
tune	1	kicker+FFT	3×10^{-4}

LINAC MODIFICATIONS

Both peak current and maximum energy of the present linac have to be increased to 80 mA and 900 MeV respectively. The present low values for the emittance should remain unaffected. To that purpose the injector and the RF modulator stations will be modified; an energy spectrum compressor (ESC) added to the linac to restore the deteriorated energy spectrum.

INJECTOR: HRC[6] redesigned the injector. It appeared feasible to increase the current fivefold without a significant deterioration of the emittance; this could be achieved with only minor changes of the optical components.

MODULATORS: raising the energy to 900 MeV requires an increase in RF power from 60 to 130 MW. Therefore the present 5 MW 2.5 % RF d.f. klystrons will be replaced by a tube which can deliver 10-20 MW at 0.15 % RF d.f.[7].

This tube will initially operate at a 10 MW RF output level. The video power will be obtained from the present pulse forming network modules by connecting them in parallel instead of in series [7].

BEAM BREAK UP: studies by HRC [6] indicate that beam break up will not be a problem for peak currents up to 80 mA assuming the previously mentioned 10 MW RF power levels.

ESC: the peak current increase will cause an increase of the energy spread from 0.3 % to about 1 %. This value is beyond the acceptance of the ring so an ESC has to be implemented. A full description of the ESC system is given in [8].

BSY: the BSY should be able to handle electron energies of 900 MeV instead of the present 550 MeV. The system has been redesigned while preserving its excellent optical quality [9]. All quadrupoles can be re-used. The dipole magnets will all be replaced.

TIMESCHEDULE, MANPOWER AND BUDGET.

The realization of the project is scheduled to take 4 years. Civil engineering, the implementation of the ESC and the upgrade of the BSY will be completed early 1990. Ordering and manufacturing of major systems will start mid-1989. Installation and subsystem tests are foreseen in 1990/1991. Early 1992 commissioning of the ring in stretcher mode should start. The IT will be implemented afterwards.

During the construction of the ring, operation of the present MEA facility will be reduced to 50 %.

The manpower estimate amounts to 140 effective manyears. NIKHEF's technical staff consists of 100 scientists, engineers and technicians. The total budget for the project is 26.5 M Dfl incl. VAT (~M \$ 12.6).

ACKNOWLEDGEMENTS

The work described in this paper is part of the research program of the Nuclear Physics section of the National Institute for Nuclear Physics and High-Energy Physics (NIKHEF-K), made possible by financial support from the Foundation for Fundamental Research on Matter (FOM) and the Netherlands Foundation for Scientific Research (NWO).

REFERENCES

- [1] C.de Vries e.a., The 500 MeV electron-scattering facility at NIKHEF-K. Nucl.Instr.Meth.,223 (1984) 1
- [2] R.Maas e.a., The Amsterdam Pulse Stretcher IEEE Trans. on Nucl. Sci.,NS-32,No.5,page 2706.
- [3] R.Maas and Y.Y.Wu, "Optics of the Amsterdam Pulse Stretcher", IEEE proceedings of the Particle Accelerator Conference, Chicago, March 20-23, 1989.
- [4] N.Kalantar-Nayestanaki, "A Study of the Beam-Target Interactions in a Storage Ring", NIKHEF-K/IT/89-01.
- [5] Private communications with A.Poncet (Cern) and H.J. Halama and A.van Steenbergen (NSLS, Brookhaven)
- [6] Haimson Research Corporation, Palo Alto, Cal., U.S.A.
- [7] F.B.Kroes and E.Heine, "Modification of MEA modulator-klystron units enabling short pulse injection into a pulse-stretcher ring", IEEE proceedings of the Particle Accelerator Conference, Chicago, March 20-23, 1989.
- [8] J.G.Noomen and R.Maas, "An Energy Compressing System for the Amsterdam Pulse Stretcher", IEEE proceedings of the Particle Accelerator Conference, Chicago, March 20-23, 1989.
- [9] J.B. van der Laan, "New 'AFBU' beam switch yard", NIKHEF-K/APS/88-07

R. Maas and Y.Y. Wu

NIKHEF-K

P.O. BOX 4395, 1009 AJ Amsterdam, The Netherlands

1. Summary

The AmPS machine [1] has been designed as a dual-purpose machine: it will be used both as a Pulse Stretcher (PS) and as a storage ring for electrons. In the latter mode the stored beam will be used in conjunction with an internal (jet) target. Since the internal target will limit the lifetime of the beam to minutes, the storage requirements (e.g. vacuum) will be modest. In PS mode the energy range is 250 - 800 MeV; in storage mode the range is extended to 900 MeV. It is anticipated to store a current of up to 200 mA.

2. Lattice

The machine lattice consists of four curved sections, connected by dispersion-free straight sections. Each curved section comprises four identical cells of the following structure (Q is quadrupole, S is sextupole; subscripts refer to the two transverse planes):

$$(Q_{h1})-(S_h)-(Bend)-(Q_v)-(S_v)-(Bend)-(Q_{h1})$$

The phase advance of each cell is 90° in both planes, i.e. $\nu_x = \nu_y = 0.25$; the curved section, therefore, is achromatic. In this structure the two sextupole families can be set such, that all 2nd-order geometric and chromatic aberrations vanish identically (2nd-order achromat [2,3]). The dispersion function reaches its maximum value (2.7 cm / %) in the centre of the curved section. The length of the central orbit in the curved section is 20.8 m. Machine functions are given in Fig.1.

Each (achromatic) straight section comprises two matching cells; the beta functions increase gradually over the length of the matching cell, see Fig.2. The structure of a matching cell is:

$(Q_{h1})-dr_1-(Q_{v1})-dr_2-(Q_{h2})-dr_3-(Q_{v2})-dr_4-(Q_{h3})-dr_5-$
 dr_n indicates a drift space; quadrupole Q_{h1} is shared with the curved section, see above. Both the injection area and the extraction area are situated in the region where β_x reaches its maximum value (i.e. in dr_3), thus avoiding undue tolerance requirements in injection and extraction hardware. Both the RF cavity (or cavities, see below) and the internal target will be

located in dr_1 (of different matching cells), since the β -functions in both transverse planes are small in this region. Tunes of the matching cell are $\nu_x = 0.4546$ and $\nu_y = 0.4025$; the tunes of the machine in PS mode, therefore, are $\nu_x = 7.637$ and $\nu_y = 7.22$. In storage mode the tunes are slightly different: $\nu_x = 7.61$ and $\nu_y = 7.15$. The length of the machine is 211.6 m ($\tau_{rev} = 0.71 \mu s$).

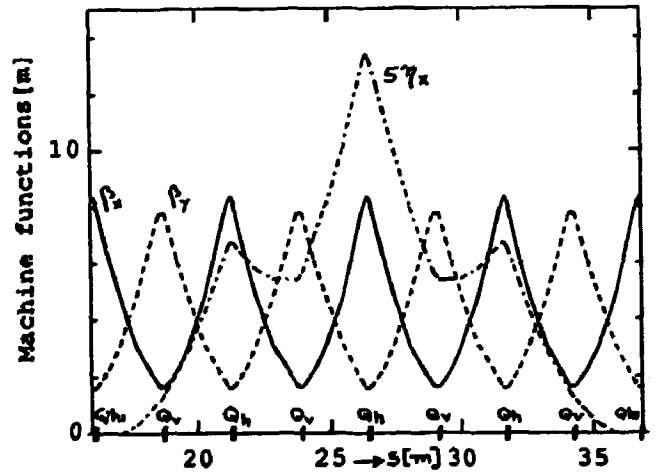


Fig. 1 Machine functions in curved section.

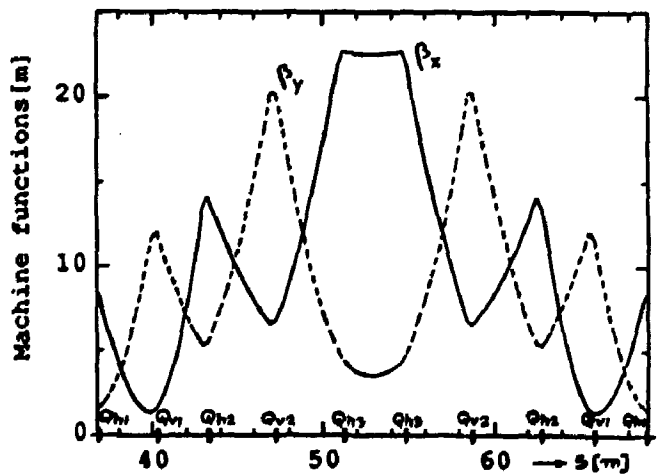


Fig. 2 Machine functions in straight section; each straight section consists of two matching sections.

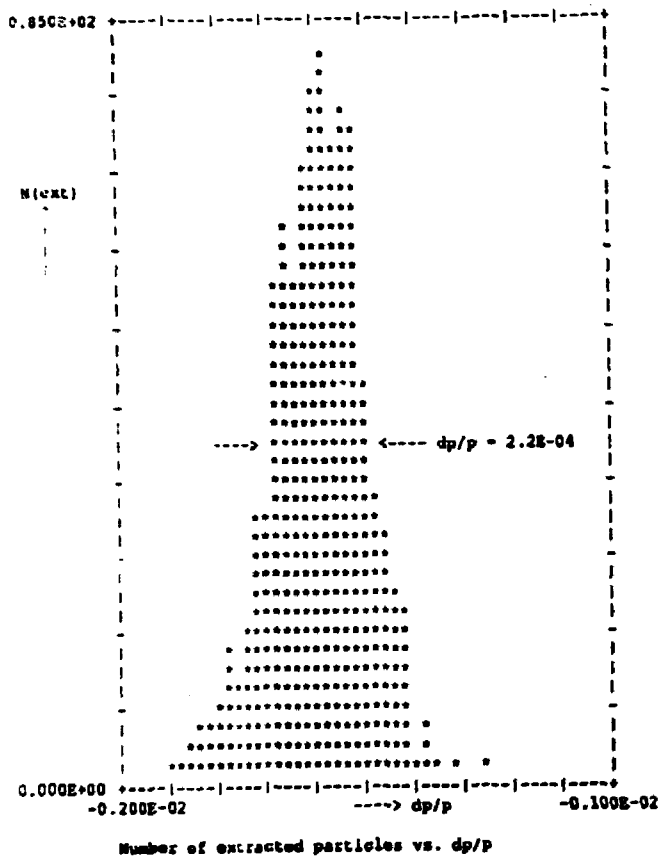


Fig. 5 Energy width of extracted beam at E = 500 MeV.

Misalignment simulations indicate possible CO deviations of up to 7 mm from the machine centre; in order to reduce these unwanted beam excursions to the level of 0.5 mm, an orbit correction scheme will be implemented. In total 32 pairs of x-y steering coils and stripline monitors (combined x-y) will be distributed around the ring (4 units in each curve; 4 units in each straight section).

4. Storage Mode operation

In order to ensure for a stored beam a quantum lifetime of the order of minutes, the height of the bucket should be at least 5 times that of the bunch [6]: $\tau_q = (e^x / 2x) \tau_e$, $x = b^2 / 2$, $b = \sigma_y / \sigma_z$. σ_b and σ_z are bucket height and bunch height respectively; τ_e is the damping time to reach σ_z . In case E = 900 MeV ($\tau_e = 36$ ms, $\sigma_z = 0.043$ %), $V_{RF} > 400$ kV for $b > 5$. In order to avoid such excessive RF requirements, it has been decided to use a lower frequency (e.g. $f = 476$ MHz) in storage mode; for the same requirements as given above, the required RF voltage in case $f = 476$ MHz is only 85 kV.

The program ZAP [7] has been used to study single bunch and coupled bunch instabilities. In order to calculate current thresholds, one needs to know the value (and frequency

behaviour) of the longitudinal coupling impedance $|Z_p/n|$ of the machine. As real data are not yet available, we assumed: $|Z_p/n| = 10 \Omega$. Also, values of both shunt impedances and Q-values of the higher-order modes (and the fundamental one) of the RF cavity are needed. The code Urmel-t [8] was used to obtain these data. Preliminary results (the cavity design has still to be optimized) indicate the following values for the max. stored current:

Table 1 Current thresholds (total average current) for longitudinal coupled bunch instabilities; (values between brackets have been calculated assuming no bunch lengthening)

E [MeV]	I_{th} [mA]
300	150 (20)
500	70 (30)
700	50
900	100

Acknowledgements

The work described in this paper is part of the research program of the Nuclear Physics section of NIKHEF, made possible by financial support from the Foundation for Fundamental Research on Matter (FOM) and the Netherlands Foundation for Scientific Research (NWO).

REFERENCES

- [1] G. Luijckx et al., The Amsterdam Pulse Stretcher Project (AmPS), Proceedings of the 1989 IEEE Particle Accelerator Conference, Chicago
- [2] K.L. Brown, A Second-Order Magnetic Optical Achromat SLAC-Pub 2257 (Feb 1979).
- [3] David C. Carey, Why a Second-Order Magnetic Optical Achromat works - Nucl. Instr. & Meth. 189 (1981) 365
- [4] L. Dallin - private communication
- [5] DIMAD, R.V. Servranckx et al., SLAC Report 285, May 1985
- [6] M. Sands, The Physics of Electron Storage Rings; an Introduction (Sect. 5.8) - SLAC-121 (1970)
- [7] ZAP - M.S. Zisman, S. Chattopadhyay and J. Bisognano, Dec. 1986
- [8] Urmel-t - T.Weiland, DESY, Hamburg

Modification of MEA modulator-klystron units enabling short pulse injection into a pulse-stretcher ring

F.B. Kroes, E. Heine, NIKHEF, P.O. Box 4395, 1009 AJ Amsterdam, The Netherlands

Abstract

In order to modify the present 500MeV, 1% duty factor electron accelerator MEA into a 900MeV, 0.1% d.f. injector for a newly to be build pulse-stretching ring, the present modulator-klystron units have to be adapted from 4MW, 2% d.f. mode of operation into the 10MW, 0.2% d.f. mode.

Suitable klystrons are commercially available, the matching modulators, however, will be obtained by modifying the present ones, which policy is dictated by economical considerations.

The design principles of these modulators -a proto-type is presently under construction- will be discussed. Special attention is given to the video-pulse shape requirements, dictated by the future performance of the pulse-stretcher. This device has to deliver low emittance, high duty factor (~90%) beams for nuclear physics experiments.

Some proto-type tests of the video-pulse forming modifications will be presented.

Introduction

At NIKHEF-K elaborate (e,e') and (e,e'X) experiments are carried out with 500 MeV, 1% d.f. electron beams from the Medium Energy Accelerator (MEA). In order to extend this programme especially towards double and triple coincidence experiments, the d.f. and max. energy of the beam have to be increased to 90% resp. 900MeV. The d.f. increase will be obtained by means of a pulse-stretching ring, called UPDATE (ref.1), presently under construction. The accelerator will then serve as an (3-turn) injector for this 200m. long ring. This implies that the beam pulse length has to be decreased from 30µs to 2.15µs and that the r.f. peak power has to increase considerably. Moreover, due to the drastic decrease in d.f. the peak currents to be accelerated should increase from 20mA to 80mA in order to maintain average currents at the target at a reasonable level.

Table 1 presents the main machine parameters in the present and in the future operation mode. Table 2 presents the specifications of the Varian klystrons (VA938D), presently in operation and those of the newly to install Thomson klystrons (TH2129), which have been chosen to provide the lower d.f. (0.2%) and increased r.f. peak power (10MW). In the next paragraph will be described how the present modulators will be modified to accommodate the TH2129 klystrons.

Table 1 Accelerator parameters before and after conversion into an injector for UPDATE

Mode of operation		present	future
Energy (o mA)	MeV	540	827
Peak current	mA	20	80
Beam loading	MeV/mA	2.8	2.5
Beam pulse length	µs	30	2.15
Repetition rate	Hz	300	400
Average current	µA	>100	70
Klystron R.F. peak	MW	4	10
Number of klystrons		12	12
Energy spread	%	0.3	1. a)

a) For proper injection into the stretcher ring, the energy spread will be decreased to 0.1% by means of an energy-spectrum compressing system (ref. 2)

Table 2 Klystron specifications

		present VA 938D	future TH2129
R.F. peak power	MW	4	10. a)
average power	kW	100	30
pulse width	µs	40	4
rep. rate	Hz	500	500
duty factor	%	2	0.2
drive peak power	W	<100	<100
BW (-0,5 dB)	MHz	20	10
Cathode voltage	kV	120	170
current	A	85	140
duty factor	%	2.5	0.3
Collector diss.	kW	350	100
Efficiency	%	43	43

a) the TH2129 is capable to deliver 15 MW

Modulator modification

Before describing the modification, the main features of the existing modulators, which have been described in detail in ref.3 and 4, will be presented here.

The existing modulator lay-out is shown in fig.1.

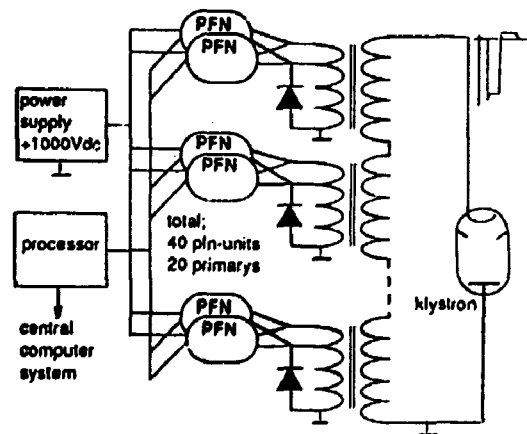


fig.1. Modulator lay out

There are 40 pulse forming network (PFN) units, each of which is a 2kV, 50µs line type modulator (see fig.2). As shown in fig.1 the PFN units are connected in pairs to the primary of a special multi-core pulse addition transformer. This PFN system permits the generation of klystron pulses, the amplitude and repetition rate of which can be changed by choosing (computer controlled) the number of PFN units to discharge.

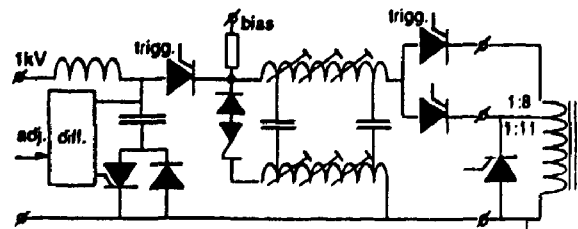


fig.2. PFN-unit

High pulse repetition rate can thus be obtained -at reduced peak power levels- by sequential switching a limited number of units at correspondingly lower repetition rate. The charging and discharging proces of the separate units is controlled by a processor. The transformer primaries not used in the discharging proces are shortened. Fig.3 shows the 3 different discharging schemes presently in use for 1, 2 and 4MW peak power levels.

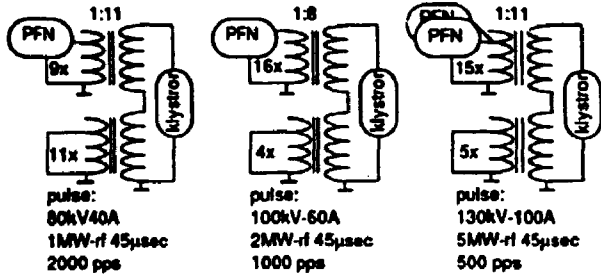
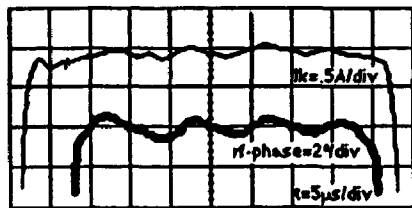


fig.3. Discharging schemes for 1, 2 and 4MW

An example of the flat-top behaviour of the r.f. pulse at the output of the VA 938D klystron is shown in fig. 4. The ripple is in the order of 0.3% for 45µs pulse width.

fig.4
Pulse flatness and phase measurement at 2MW rf level. (109kV-64A)



However, as we will show below, the fall-time of this pulse is about 10µs due to the large leakage inductance of the pulse transformer which, although acceptable for the 45µs pulse width, should be appreciable shortened for the 4µs flat-top pulses required after modification.

Considerable investments have been made in the existing batch of twelve 1% d.f., 4MW modulator-klystron units. Therefore, a design study has been started to investigate how the conversion of the MEA accelerator into a short pulse injector for the pulse stretcher could be carried out economically. As mentioned before, the VA938D klystrons have to be replaced by a new type suitable for the low d.f. (0.2%), high peak power (10MW) requirements. The present modulator, however, can be adapted by relatively small changes in the PFN network as we will discuss now.

Four main points have to be considered when adapting the PFN unit network:

- Improvement of the short-circuiting behavior
- Pulse shortening from 45µs to 4µs flat top
- Matching of the new klystron impedance to the modulator
- Increase of the input power level to obtain the 10MW r.f. from the new klystron.

The short circuiting behavior can be improved considerable by connecting a "short circuit thyristor" to the primary of the pulse transformer (see fig.5).

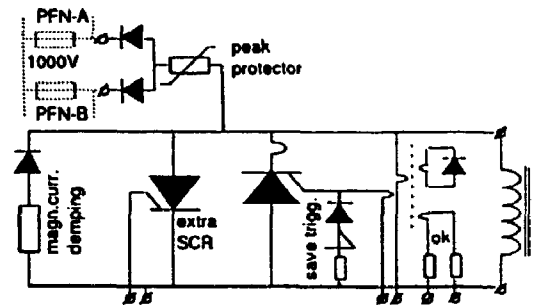
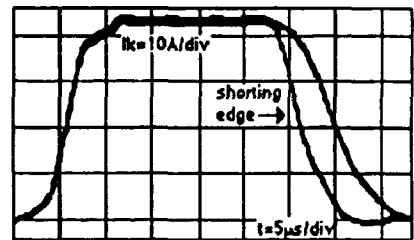


fig.5. Primary shorting circuit

This thyristor can always be triggered during the trailing edge of the pulse and will result (see fig.6) in a steeper trailing edge or shorter falltime. Moreover, positive reflections can be converted into negative reflections so that the PFN is always to be charged from the end dictated by the end of line clipper. Mismatch is allowed within the dissipation limits of the end of line clipper.

The thyristor can also be triggered when the klystron arcs. Then the pulse is short circuited at the primaries and the arcing energy will be limited. Both thyristors are triggered by an external gate pulse to prevent them against damage by the di/dt of the pulse.

fig.6.
Short circuiting of a primary. (25µsec test pulse)



Pulse shortening and proper matching to the newly to install klystron has been obtained, in the modulator test-facility, by rearranging the PFN network as shown in fig.7.

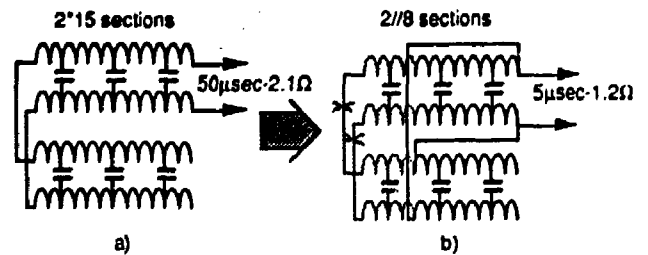


fig.7. Pulse forming network
a) before modification
b) after modification

Using these modified PFN units the 10 MW r.f. peak power can be reached as shown in the discharging schemes presented in fig.8.

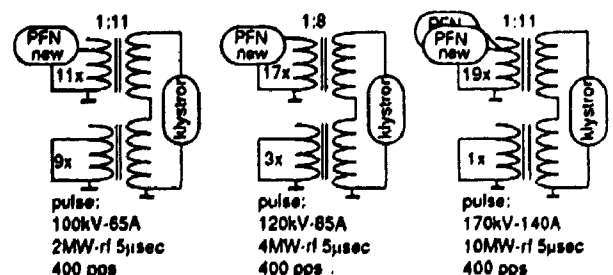


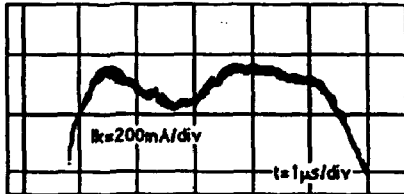
fig.8. Discharging schemes for 2, 4 and 10MW using modified PFN-units

Operation at just the 10MW level (170kV) does not provide enough pulse-level range control for the conditioning of the klystrons and the beam energy of the accelerator. Therefore, as is the case in the present situation, the different switching schemes shown in fig.8 will be essential also for the modified klystron-modulator units. With these schemes an almost smooth input power level range from 90kV-50A to 180kV-150A can be achieved.

Note that the processor must be able to cope with more primary PFN unit choices for discharge than is the case with the present modulator.

Using a limited number of modified PFN units installed in the modulator test facility the 4 μ s flat-top (= 0.3% ripple) behavior is obtained is shown in fig.9.

fig.9
Pulse flatness of modified PFN at 52A klystron current

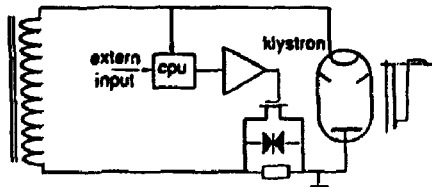


On the basis of these test results it is expected that with the modified modulator-klystron units and considering the considerable increased beam current level requested for the pulse-stretcher, the energy spread of the beam will be in the order of 1%. This spectrum has to be reduced to the 0.1% level for proper injection into the ring, which will be achieved by a so-called energy spectrum compressor system (ref.2) beyond the accelerator. Nevertheless it seems worthwhile to consider to what extent the 1% energy spectrum from the accelerator itself can be reduced.

To this purpose we have started a development which involves pulse top level stabilization.

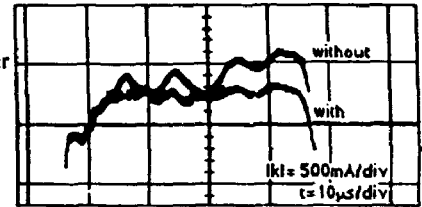
A power FET has been installed in series with the present klystron on the low voltage side of the pulse transformer (fig. 10).

fig.10
Principle of pulse top level stabilization



First test result is given in fig.11, showing a considerable improvement of the flat-top behavior.

fig.11
Flat top behaviour without and with power FET



Conclusion

At this stage of the development programme it seems likely that the adaptation of the present modulators for use of the MEA accelerator as an injector for the pulse-stretching ring can be achieved. This implies that a considerable part of the present batch of 12 modulators will still be usable. Further studies are in progress.

Acknowledgement

We gratefully acknowledge the valuable contributions of the whole NIKHEF-K technical staff in the designing and constructing stage.

The work described in this paper is part of the research program of the National Institute for Nuclear and High Energy Physics (NIKHEF), made possible by financial support from the Foundation for Fundamental Research on Matter (FOM) and the Netherlands Organization for Scientific Research (NWO).

References

- 1) R. Maas et al., "The Amsterdam Pulse Stretcher", IEEE Trans. on Nucl. Sci. NS-32 (1985) 2706
- 2) J.G.Noomen et al., "An Energy Compressing System for the Amsterdam Pulse Stretcher", This conference
- 3) P.J.T. Bruinsma, E.Heine et al., "An all solid state line-type modulator", IEEE Trans on Nucl. Sci. NS-20(1973)
- 4) P.J.T. Bruinsma, F.B. Kroes et al., "The 500 MeV, 2.5% duty factor linear electron accelerator (MEA)", IEEE Trans. on Nucl. Sci. NS-30 (1983) 3599
- 5) G.Luijckx, P.J.T.Bruinsma et al, "The Amsterdam Pulse Stretcher Project (APS)", This conference

Performance and Modification of the MEA R.F. Drive System

F.B. Kroes, T.G.B.W Sluyk, B. Heutenik, NIKHEF, P.O. Box 4395,
1009 AJ Amsterdam, The Netherlands

Abstract

The twelve modulator-klystron units serving the 500 MeV linear electron accelerator (MEA) (ref. 1) will be modified to convert the accelerator into a 900 MeV, 0.2% d.f. injector for the pulse stretcher project, presently under construction (ref. 2). The new klystrons needed for this purpose have to be provided with higher input R.F. peak power, which implies modification of the present R.F. drive system. This modification also involves the inclusion of fast R.F. PIN diode switches in the R.F. drive system of each klystron to enable spreading of the R.F. timing of the twelve stations. This is essential - given the much shorter pulses requested for injection into the pulse stretcher - to suppress the transient beam loading effect. Design consideration for the modification of the MEA R.F. drive system and initial tests will be presented.

1. Introduction

The present 500 MeV electron accelerator delivers 2% d.f. beams at a maximum energy of 600 MeV to the experimental area, where an elaborate nuclear physics programme involving single arm (e,e') and coincidence (e,e'X) experiments is carried out. In order to extend this programme in the future, the d.f. and the max. energy of the beam will be raised to 90% and 900 MeV respectively. To this purpose a pulse-stretcher ring is under construction for which the accelerator (MEA) will serve as a 900 MeV, 0.2% d.f. injector.

Due to the d.f. decrease of the accelerator itself the peak current to be accelerated has to increase from 10 mA to 80 mA to extract acceptable average currents from the pulse-stretcher.

As is discussed elsewhere in this conference (ref. 3) the modulator-klystron units, which provide the R.F. peak power for the accelerator, have to be modified.

The present 2%, 4MW klystrons (VA 938D) will be replaced by 0.2%, 10 MW tubes (TH 2129). Table 1 lists the main R.F. specifications of these two klystron types

Table 1 Main klystron specifications

		Present VA 938D	Future TH 2129
Peak power	input	70	100
	output	4	10 ^{0.2}
Pulse width	μ s	40	4
Repetition rate	Hz	500	500
Average input power	W	7	0.7

a) The TH 2129 is capable of delivering 15 MW peak power

Obviously the present R.F. drive systems have to be modified rather drastically to accommodate the newly to install klystron. In addition, related with the much shorter pulse width, provisions have to be made to compensate for transient beam loading. Namely, the current content of the beam pulse during the 1.3 μ s fill time of the accelerator sections represents a considerable fraction of the total current in the 2.1 μ s beam pulse requested for (three turn) injection in the pulse stretcher.

Compensation of this transient beam loading will be established by spreading starting times of the R.F. pulse for each klystron. This feature requires the introduction of a high peak power PIN diode pulse shaper. In the following section we will briefly discuss the lay-out and performance of the present R.F. drive line system. The design considerations and some initial test of the newly to install R.F. drive system will be given in section 3.

2. Present R.F. drive line system

The lay-out of the R.F. drive line providing the 12 klystrons with R.F. input power is shown in fig. 1.

The R.F. c.w. signal from the 2856 Mc synthesizer is AM modulated to a pulse width ranging from 0.1 to 40 μ s and then amplified in two steps to 300 W, which power is driving the first klystron.

The main part of the 2 MW output power from this klystron is used for feeding the buncher and first section of the accelerator. By means of a 18 dB coupler in conjunction with an attenuator, 15 kW of this power is fed into the 200 m. long ultra-stable rectangular wave guide installed in parallel with the accelerator itself. For each of the remaining klystrons 350 W drive power is coupled out from this drive-line. The coupling ratio of these couplers are ranging from -17dB at the second klystron to -10dB at the last klystron. For optimum performance of the accelerator special care has been taken to keep the droop and ripple of the video pulse of the transmitter of the first klystron within 0.2% over at least 35 μ s. Furthermore the wave-guide drive line is temperature and absolute pressure controlled ($\pm 0.03^\circ$ C, resp. ± 1.5 Torr) resulting in a R.F. phase stability within one electrical degree. The drive-line envelope and support are shown in fig. 2. Each klystron has its own R.F. drive system containing a solid state attenuator (SSA) and a digital phase shifter (DPS) which are electronically controlled.

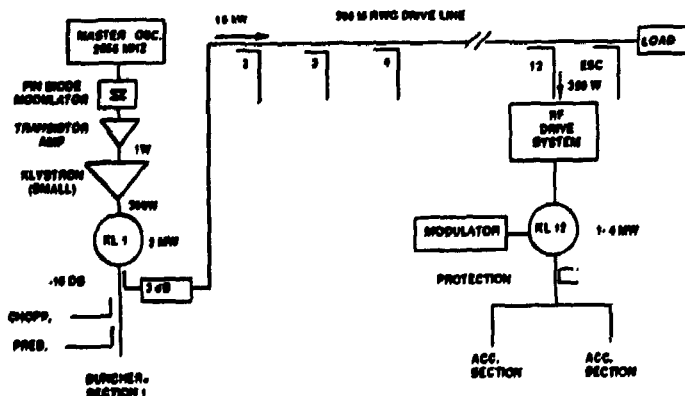


fig. 1 Layout of the accelerator RF system

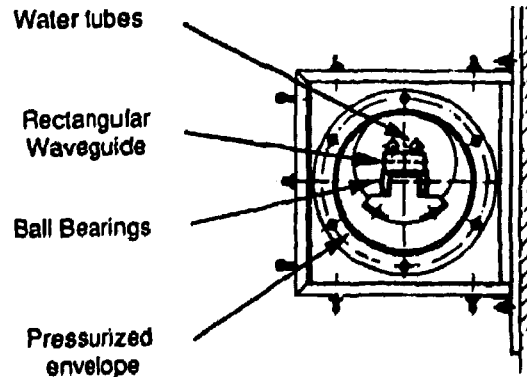


fig. 2 Driveline envelope and support

The Solid State Attenuator (SSA)

The inhouse developed SSA controls on a pulse to pulse basis the klystron drive power -which ranges from 25 to 100 W- for operation at 1, 2 and 4 MW R.F. output peak power levels.

The SSA sets 200 μ s in advance the correct R.F. input power before the next pulse is fired.

The device has a flat attenuation response (< 1dB) during the pulse. Its phase remains during the 40 μ s pulse constant within 1 degree. Also the long-term stability of the phase is excellent. Although rather insensitive to temperature changes temperature control at 45 $^{\circ}$ C is applied for long-term stability. The SSA can handle 350 W R.F. peak power for 40 μ s pulse length.

Some main specifications are given in Table 2

Table 2 Solid State Attenuator (SSA) specifications

range for flat pulse attenuation	10	dB
insertion loss	2.5	dB
phase vs temp	1	degree / $^{\circ}$ C
input power at 50 μ s / 4000 μ s	350	W
speed	10	μ s
off-state isolation	-35	dB
input and output reflection	-25	dB
output variation during pulse at various attenuator settings	.5	dB

The printed circuit lay-out of the SSA is shown in fig. 3.

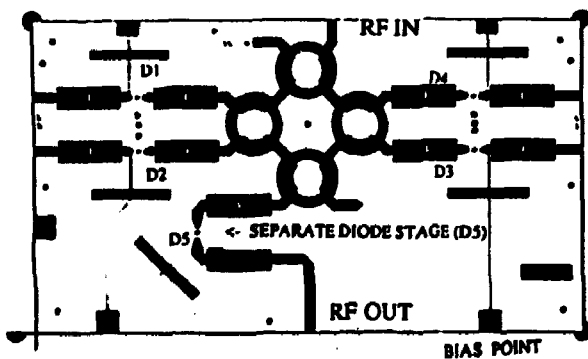


fig.3 Attenuator PCB layout

The Digital Phase Shifter (DPS)

The DPS installed in the MEA klystron drive systems is commercially available. Table 3 presents its main specifications.

The device is a non-reciprocal latching waveguide ferrite phase shifter. It has 32 phase states (360 deg. 5 bits) from 0 to 348.75 degrees in 11.25 degree steps with low insertion loss (typically 0.9 dB). The accuracy is about 2 degrees. The possible switching speed is 2500 events per second. The phase/temperature sensitivity was measured to be 1 degree -phase / $^{\circ}$ C. Therefore the device is kept at a constant temperature of 45 $^{\circ}$ C.

Table 3. Digital Phase Shifter (DPS) specifications

insertion loss	1	dB
phase vs temp	2	degree / $^{\circ}$ C
input power at 50 μ s / 400 μ s	350	W (peak)
speed	2000	μ s
insertion loss variation due to phase stepping	0.3	dB

Computer interfacing and protection electronics

Computer interfacing as well as control of the SSA and DPS units is carried out by elaborate control and protection electronics. The protection circuit takes care of monitoring and interfacing signals such as from different cooling- and vacuum circuits of relevant accelerator components and from standing wave ratio monitors.

If these signals give cause for disconnecting the R.F. power this can be achieved within 7 μ s (beam pulses may be as large as 40 μ s!) in two steps. First the SSA is set to maximum attenuation (20 dB). Because of the high gain of the klystron, the power has to be further reduced by 30 dB, for which purpose a separate diode is incorporated in the circuitry of the SSA (see fig. 3, diode 5).

3. Modification of the R.F. drive system requested for the pulse-stretcher mode of operation

Apart from the higher peak R.F. drive power level required (see table 1) the main modification is to enable the compensation of the transient beam loading (ref. 4). It is essential to achieve this compensation because due to the much shorter beam pulse (2.15 μ s) the effect of transient beam loading during the 1.3 μ s filling time of the accelerator sections is dominantly present. As has been shown in ref. 5 compensation can be established by spreading the starting time of the individual klystron r.f. pulses. In order to control the timing trigger of the individual R.F. drive system units relative to each other, fast R.F. PIN diode switches are incorporated in the R.F. drive systems as indicated in the block diagram presented in fig. 4.

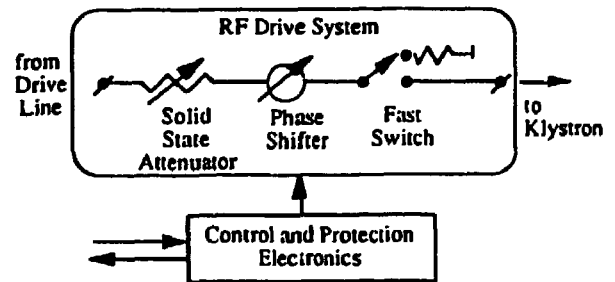


fig.4 : Block diagram of R.F. Drive System

Fast R.F. PIN diode switch

For the transient beamloading compensation project a fast R.F. PIN diode switch is developed. The main specifications are given in table 4.

The first switch is tested in the prototype R.F. drive system under continuous operation conditions. The fast R.F. PIN switch makes it possible to give each of the twelve stations its own R.F. pulse start. The employed fast switch is able to do "hot" switching which means: switch on in the presence of RF-drive power from the Drive-Line (> 150 W, 50 μ s). The obtained speed is faster than 100ns (rise time). Some protection circuits are build in the R.F. drive system. These are used to prevent the trailing edge of the PIN switch to occur during the R.F. pulse. This gives reduced power dissipation in the switching diodes and failsafe operation.

Table 4. Specifications of the Fast R.F. Switch

insertion loss	1	dB
phase vs temp	0.5	degree / $^{\circ}$ C
input power at 50 μ s / 400 μ s	150	W (peak)
at 2 μ s / 3 ms	250	W (peak)
speed 10-90%	100	ns

Test measurements

For the purpose of the future modification of the R.F. drive systems for the newly to install klystrons a prototype R.F. drive system including the fast R.F. PIN diode switch has been build.

Test measurements with this system have been carried out. Some results will be discussed now.

Figure 5 shows the flatness of the R.F. output of the Drive System for several settings of attenuation. A flat pulse is needed for a low spread in electron energy. The power variation is further reduced by the klystron which works in saturated mode. Since the beam starts at a later point in time than the R.F. pulse, the level is stabilised to within 0.1 dB.

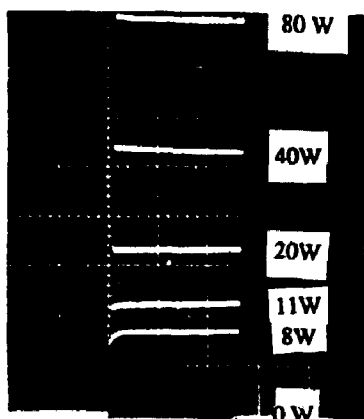


fig.5 R.F. drivesystem output flatness for several attenuation settings. (time 20µs/div)

At the same time an excellent phase flatness of 0.2° is achieved. Figure 6 shows the delayed switching response of the build in Fast Switch. (see spreading time technique) The starting point can be set at any point within the pulse. The falling edge of the Fast Switch is always delayed until after the R.F. driveline pulse to lower the switching power in its diodes.

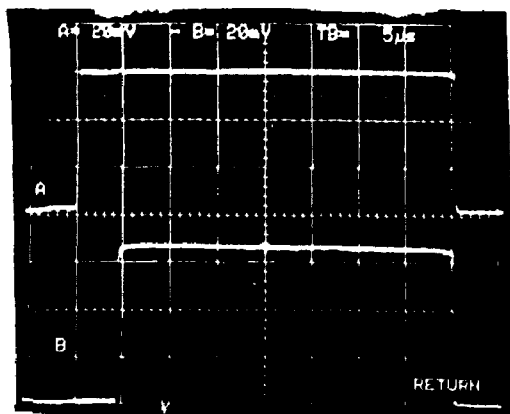


fig.6 Delayed switching of the R.F. Switch using a long pulse. (timescale: 5µs/div, vertical: relative R.F. power) A= input drivesystem, B= output drivesystem

Spreading time technique

The prototype of the modified R.F. drive system has been incorporated in one of the stations along the accelerator (number 10).

In order to carry out preliminary tests of the spread R.F. timing mechanism and its influence on the energy spread of the beam the following test has been carried out.

Only the first two modulator-klystron stations (in the following mentioned as injector station) and station Nr. 10 have been used for acceleration. The energy of the beam after the injector station is about 50 MeV and further increased by station 10 to about 97 MeV. The peak current was 5 mA and the beam pulse width 2.0µs. The beam loading term of the accelerator is 2.8 MeV/mA, the fill time of the acceleration structures is 1.3µs. Three experiments are carried out under the following starting time conditions.

Firstly, keeping the starting times of the R.F. pulses from the injector station and station 10 the same, the beam pulse was triggered > 1.3µs later. (exp. 1). This is the usual condition of the present (long R.F. pulse) mode of operation.

Secondly (exp. 2) the starting time of the R.F. pulses of both the injector station and station 10 were simultaneously delayed such that it occurred within 1.3µs before the start of the beam pulse. Finally (exp. 3) the starting R.F. time of station 10 was further delayed relative to that of the pulse from the injector station but still occurring within 1.3µs before the start of the beam pulse. The control accuracy of the different triggers has been 0.1 µs.

In order to study the influence of these spreading time conditions on the beam energy spread, the beam energy and the lowest and highest energy involved in the accelerator beam pulse have been measured with the tune-up line beyond the accelerator. A secondary emission monitor, serving as an energy spectrum analyser is incorporated in the tune-up line. Those measurements give for the three spreading time conditions mentioned above the following results:

Table 5. Results of the tests with spreaded R.F. timing.

		Exp. 1	Exp. 2	Exp. 3
Beam Energy (steady state)	MeV	97.1	97.1	97.1
Highest energy detected	MeV	112.9	105.2	99.4
Lowest energy detected	MeV	98.3	98.3	98.3

The energy spread in the first experiment, 14.6 MeV, corresponds with the accelerator beam loading term (2.8 MeV/mA). It is apparent that the spreading time experiment shows a dramatic improvement of the energy spectrum of the 2µs beam pulse. The results are convincingly enough to expect that -by incorporating the fast PIN diode switch techniques in all stations - high energy beams (more active accelerator stations) will show an energy spectrum well within the 1% acceptance of the energy spectrum compressor (see ref. 6) to be installed beyond the accelerator.

Acknowledgement

We gratefully acknowledge the valuable contributions of the whole NIKHEF-K technical staff in the designing and constructing stage.

The work described in this paper is part of the research program of the National Institute for Nuclear and High Energy Physics (NIKHEF), made possible by financial support from the Foundation for Fundamental Research on Matter (FOM) and the Netherlands Organisation for Scientific Research (NWO).

References

- 1) P.J.T. Bruinsma, F.B. Kroes et al., "The 500 MeV, 2.5% duty factor linear electron accelerator (MEA)", IEEE Trans. on Nucl. Sci. NS-30 (1983) 3599.
- 2) -R. Maas et al., "The Amsterdam Pulse Stretcher", IEEE Trans. on Nucl. Sci. NS-32 (1985) 2706
-G.Luijckx, et al., "The Amsterdam Pulse Stretcher Project (APS)", This conference.
- 3) F.B. Kroes, E. Heine, "Modification of MEA modulator klystron units enabling short pulse injection into a pulse-stretcher ring", This conference.
- 4) Linear accelerators (ed. Lapostolle, Septier (1970): J.Haimson "High duty factor electron linear accelerators"
- 5) B. Aune et al., "Transient beamloading calculations and experiment at the SACLAY electron linac", IEEE Trans. n Nucl. Sci NS-30(1983) 2995
- 6) J.G. Noomen et al., "An energy compression system for the Amsterdam Pulse Stretcher", This conference.

An Energy Spectrum Compressor System (ESC) for the Amsterdam Pulse Stretcher (AmPS)

J.G. Noomen, R. Maas,
NIKHEF-K, P.O. Box 4395, 1009 AJ Amsterdam, The Netherlands

Summary

To obtain high duty (90%) electron beams, the present 2% d.f. 500 MeV linac (MEA) will be modified into a low d.f. (0.1%) injector for the pulse stretcher ring presently under construction[1]. The accelerator peak current has to be increased from 10 mA to 80 mA to obtain from the pulse stretcher an average current of 65 μ A. The resulting increase of the energy spread from 0.3% to 1 - 2% requires the installation of an energy compression system (ESC) to match the 0.2% acceptance of the pulse stretcher. The ESC consists of four magnets followed by a short-filling time r.f. traveling wave accelerator structure. Considerations concerning required energy range, beam loading, phase errors, and current ripple which determine the longitudinal dispersion and the required r.f. power source are presented.

Introduction

The energy spread of electron beams emerging from a linear accelerator can be considerably reduced by means of an energy compression system[2]. Such a system contains two parts: a magnetic channel in which the energy spread of the beam through path length differences is translated into a longitudinal phase stretching of the electron bunch and an acceleration structure in which the energy compression of the enlarged phase spread of the bunches occurs. The layout of the ESC is given in Fig.1. The four-magnet system, designed to fit in the existing acceleration vault, is based on laminated magnets to enable fast degaussing. This allows fast switching between compressing and non compressing mode. The choice of four magnets allows installation of monitoring equipment (viewing screen and a SEM grid for energy spread detection) in the center of the system. Optical considerations request the application of large pole face rotations. To reduce occurrence of second order aberrations due to pole face rotation, the magnets will be provided with field clamps. The energy spread acceptance of the system is restricted to 1.8% by a 1.8 cm diameter collimator, installed between the first and second magnet. In the following we will discuss in some detail the design considerations of the two elements of the ESC.

Choice of longitudinal dispersion value.

The accelerator will be provided with 10 MW klystrons of which the high voltage will be supplied by a line type modulator [3]. With this type of modulator a considerable contribution to the energy spread is due to the effects of high voltage ripple on the RF. The total accelerator energy spread, δ , can be calculated from,

$$\delta = f(\varphi_0, \varphi_k, \varphi_B, \varphi_c) \cdot \frac{E + E_l}{E} + \frac{E_l}{E} \cdot \frac{di}{i} \quad (1)$$

E is the energy (MeV) including beam loading, E_l is the total beam loading (2.57 MeV/mA) and di/i is the relative beam current ripple. $f(\varphi_0, \varphi_k, \varphi_B, \varphi_c)$ represents the effect of the klystron high voltage ripple (φ_k), the effective bunch width (φ_B) and the position of the bunch center (φ_c) [4]. φ_0 is the angle where RF power variation due to klystron voltage ripple is just compensated by the corresponding phase change ($\varphi_0 = 7^\circ$ in our case). φ_c and φ_0 are related to the crest of the accelerating field. The growth of the bunch after traversing the magnets is,

$$\varphi_{BD} = 360 \frac{D}{\lambda} \delta \quad (2)$$

D is the longitudinal dispersion in cm/%, and λ is the free space wavelength (0.105 m in our case).

Fig.2 shows the relation between the compression factor and the dispersive bunch part φ_{BD} , with the non dispersive bunch part φ_B as parameter. Also four working lines are given for $D=2$ cm/%, $E=600$ MeV, $i=80$ mA and $\varphi_{kc} = \pm 1^\circ$. φ_{kc} is the phase ripple of the compressor RF power. These lines have been obtained by calculating working points using (1) and (2). These points have been corrected for φ_{kc} . The working lines extend from $(\varphi_B)_{min}$ to $(\varphi_B)_{max}$. With increasing working line number the energy spread increases due to contributions according Table 1. $d\varphi_c$ is the deviation from the optimum φ_c value. With $\varphi_k = \pm 1^\circ$ corresponds a klystron high voltage ripple of 0.3%.

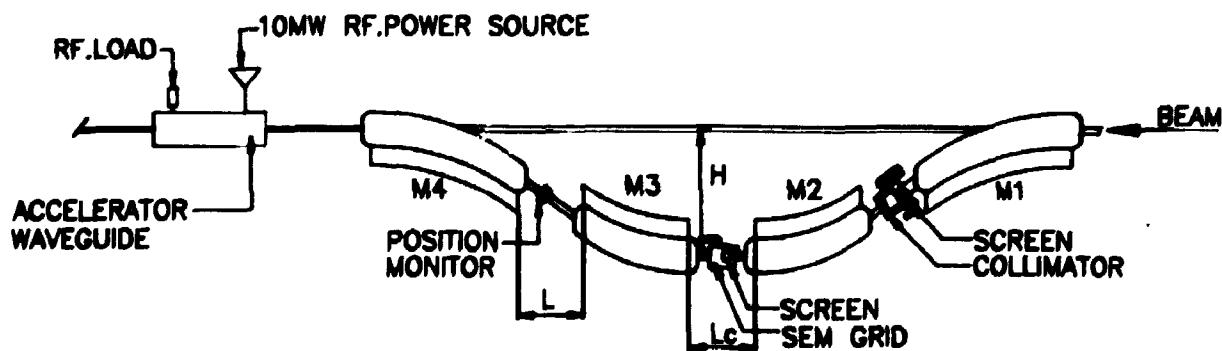


Fig.1, ESC layout.

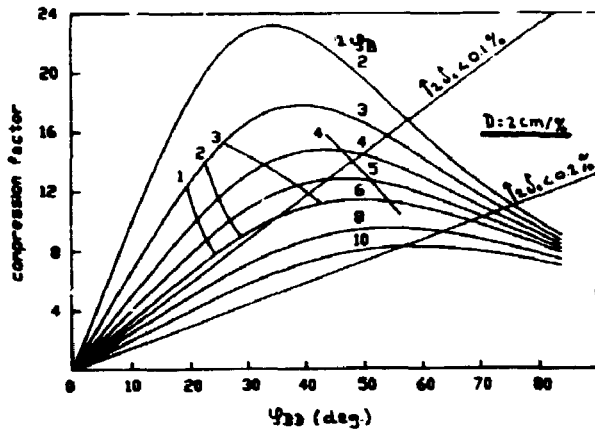


Fig. 2. Compression factor as function of dispersive bunch part Φ_{BD} . Four working lines (see Table 1) and 0.1% and 0.2% separatrices are also given (see text).

Table 1. Parameter values of working lines in Fig. 1.

line nr	$\pm \phi_c$ (°)	$\pm \phi_k$ (°)	di/i (%)
1	0	1	0
2	1	1	0
3	1	2	0
4	1	2	1

Fig. 1 shows also 0.1% and 0.2% lines. Above these lines the compressed energy spread $2\delta_c$ is better than these values and below these lines it is worse. We prefer $2\delta_c$ not to be worse than 0.1%. Consequently the working points below the 0.1% line (largest Φ_{BD} values) should be positioned close to the maximum of the compression curves. As can be concluded from Fig. 1 $D=2$ cm/% does meet this criterion fairly well.

Compressor accelerator section and RF power source

The required maximum field (E_c) of the compressor accelerator is given by,

$$E_c = \frac{\phi_e}{\sin \phi_e} \cdot \frac{\lambda}{2\pi} \cdot \frac{E}{D} \quad (3)$$

ϕ_e is the angle (rad) where the deviation from the central energy is just compensated by the compressor accelerator field. The required field is maximum when E is maximum (900 MeV, $i=0$) and ϕ_e has its corresponding maximum possible value. For $\phi_B = \phi_k = \phi_{kc} = \pm 20^\circ$ and $d\phi_e = \pm 10^\circ$, $(\phi_e)_{max} = 31.4^\circ$ [5]. Substituting these values in eq. (3) yields $E_c = 8$ MeV. The maximum energy gain of a constant gradient section is given by [6],

$$E_c = k_1 \sqrt{(P/I) - k_2 \cdot i \cdot l}$$

l is the length of the section (m) and P is the RF input power (MW). k_1 and k_2 are constants depending on the geometry of the section. To determine the required product P/I , the beam loading term (second term) can be neglected since the beam induced field is small compared with the generator field (first term) and 90° out of phase.

Assuming quality factor (Q) and shunt impedance (r) to be constant k_1 and k_2 depend only on the filling time. Numbers for P/I (at $E_c=8$ MeV) and k_2 for estimated values of $Q=13000$ and $r=50$ M Ω /m are shown in Table 2. We see that at the cost of increasing filling time the product P/I decreases. This means a shorter thus cheaper accelerator section and less RF power is required. However during the filling time an energy offset occurs due to the build up of beam induced field. For this reason we aimed for a filling time of 0.1 μ s which is short compared with the beam pulselength (2.1 μ s).

Table 2. P/I and k_2 values for $E_c=8$ MeV, $Q=13000$, $r=50$ M Ω /m

Filling time (μ s)	P/I (MW.m)	k_2 (MeV/A.m)
0.10	9.93	1.68
0.15	6.84	2.50
0.20	5.31	3.29
0.25	2.09	4.06

Taking into account 15% RF power loss in the RWG network, a 10 MW RF power source combined with a filling time of 0.1 μ s will result in a compressor section length of 1.16 m. For $i=80$ mA the maximum energy offset during the fill time due to transient beam loading is then 0.026%. Compared with the aimed energy spread of 0.1% for the whole beam pulse length this is quite an acceptable value.

Optimization of magnet size

To elongate the bunch as function of the energy spread the transfer function of the four magnet system must have a non zero (H)-element (D) and should behave in both transverse planes as a driftlength. A geometry as given in Fig. 1 fulfills these requirements. In order to reduce the total system length, we allow,

$$T_y = \begin{pmatrix} -1 & Ly \\ 0 & -1 \end{pmatrix}$$

which means a crossover in the y plane in the centre of the system. The location of the ESC restricts the value of H (see Fig. 1) therefore an optimization of the magnet system was necessary. For some longitudinal dispersion values and maximum magnetic fields of the two centre magnets results of this optimization are shown in Fig. 3.

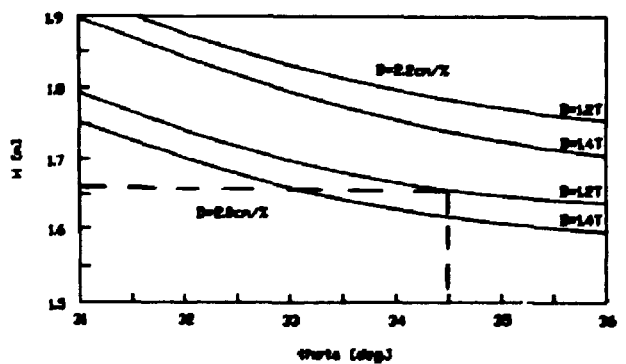


Fig. 3. Variation of H (see Fig. 1) as function of bending angle.

From this figure we conclude that Θ shouldn't be larger than 35 degrees; increasing the maximum magnetic field has a minor influence. This allows to adopt a moderate maximum magnetic field of 1.2 Tesla based upon a balance between magnetic field quality, magnet costs and electrical power costs. With Θ values below 35 degrees also second order aberrations are within tolerable limits. The longitudinal dispersion value has a much larger influence but this value is determined for other reasons as outlined above. The magnet parameters are given in Table 3.

Table 3. Compressor magnet data. M_1 & M_4 are the two outer magnets, M_2 & M_3 are the two central magnets.

	(M_1 & M_4)	(M_2 & M_3)
E_{max} [MeV]	900	900
B_{max} [kG]	8.57	12.0
ρ_0 [m]	3.502	2.502
Θ [deg]	34.50	34.50
l_c [m]	2.1089	1.5064
l_{yoke} [m]	1.9838	1.4170
g (gap) [cm]	3	3
w (pole width) [cm]	21.0	21.0
good field region [cm]	± 2.5	± 2.5
radial field homogeneity	$5 \cdot 10^{-4}$	$3 \cdot 10^{-4}$

Acknowledgement

We gratefully acknowledge the valuable contributions of the whole NIKHEF-K technical staff in the designing and constructing stage.

The work described in this paper is part of the research program of the National Institute for Nuclear Physics and High Energy Physics (NIKHEF), made possible by financial support from the Foundation for Fundamental Research on Matter (FOM) and the Netherlands Foundation for Scientific Research (NWO).

References

- 1) G. Luijckx et al., The Amsterdam Pulse Stretcher Project (AmPS), IEEE proceedings of the Particle Accelerator Conference, Chicago, March 20-23, 1989
- 2) W.H. Gillespie, M.G. Keliker, The energy compressor at the Glasgow 170 MeV electron linac, NIM 184 (1981) 285-29
- 3) F.B. Kroes, E. Heine, Modification of MEA modulator-klystron units enabling short pulse injection into a pulse stretcher ring, IEEE proceedings of the Particle Accelerator Conference, Chicago, March 20-23, 1989
- 4) J.G. Noomen, Energy Spectrum Compressor longitudinal dispersion and R.F. power source, internal report, NIKHEF-K, Amsterdam
- 5) R.E. Laxdal, Design of an energy compression system for the Saskatchewan Linear Accelerator, SAL Report No. 30, March 1980, Saskatchewan Accelerator Laboratory, University of Saskatchewan, Saskatoon.
- 6) P.M. Lapostolle, H.L. Septier, Linear Accelerators, page 151, North Holland Publishing Company, 1970